Preprints of the 19th World Congress
The International Federation of Automatic Control
Cape Town, South Africa. August 24-29, 2014

Comparison of Heuristic Controllers for an Automotive Semi-Active Suspension

Juan Carlos Tudon-Martinez * **Ruben Morales-Menendez** *
Ricardo A. Ramirez-Mendoza * **and Luis Amezquita-Brooks** **

* *Tecnológico de Monterrey, Monterrey NL, México,*
{jc.tudon.phd.mty, rmm, ricardo.ramirez }@itesm.mx
** *UANL, Monterrey NL, México, amezquita-brooks@ieee.org*

Abstract: A comparative analysis between two different heuristic suspension control strategies is presented, the approaches have been designed to control the vertical dynamics of a full size pick-up truck model equipped with Magneto-Rheological (*MR*) dampers. The control schemes to compare are: (1) a global suspension controller and, (2) four independent controllers, one for each Quarter of Vehicle (*QoV*) model; both control schemes depend only on measurements. The main idea is to compare the control performances and the implications that these heuristic controllers have. Experimental data are used to model an *MR* damper in each corner. Two tests have been used to compare the control performances when the vehicle is driven in straight trajectories: (1) a running test on a road based on the standard ISO 8606 and, (2) a road that excites the vertical dynamics at different frequencies (*Bounce Sine Sweep* test). Results obtained using CarSim^{TM} show that the comfort performance is better when the controller is well coordinated among the wheel-stations (global suspension controller); the improvement is 33% in the heave motion and 35% in the pitch angle. The *QoV*-based controller presents uncoordination that complicates the attenuation of the vehicle body movement; however, the road holding is improved.

Keywords: Automotive Semi-Active Suspension, Controller Design

1. INTRODUCTION

During last years, intelligent suspension systems have been developed to increase comfort and safety in vehicles. According to ISO 2631, people could suffer several health damages due to a constant exposure to vibrations. Thus, semi-active or active shock absorbers are a good solution to control the chassis motion and, moreover, to maintain the road holding.

When the suspension design (chassis, stabilizer bars, dampers, springs, etc.) is limited by space, the inclusion of active dampers is more complicated because its external power supply could demand considerable space. Additionally, semi-active dampers like the *Magneto-Rheological* (*MR*) ones offer fast time response and wide control bandwidth with a low power requirement.

Different methodologies have been used to design intelligent suspension control systems, e.g. the model-based control techniques by using nonlinear [Yoon et al., 2010, Poussot-Vassal et al., 2012], robust [Choi et al., 2002, Wang et al., 2005, Chadli et al., 2010] or optimal control theory, [Crivellaro, 2009]. When an accurate vehicle model or an observer/estimator are not available, heuristic control techniques could offer good results with high feasibility to be implemented [Ikenaga et al., 2010, Swevers et al., 2007, Dong et al., 2009]; however, two synchronized levels of control must be designed to improve comfort. In [Tudón-Martínez et al., 2012] a novel model-free control strategy is proposed. This strategy, named *Combinatory quasi-Optimum Damping* (*COD*) controller, determines the best solution of damping force of the four semi-active dampers by using a monitoring module in the suspension system.

This extended version of [Tudón-Martínez et al., 2012] compares the performance of the *COD* controller, which includes the coupling joints among the four corners of the vehicle into the controller design (i.e. one level of control), versus an heuristic control strategy based on independent wheel-stations, named *Independent Heuristic Control* (*IHC*) where each corner has a local controller. The main idea of this research is to highlight the advantages and implications of a coordinated global suspension control system in contrast to the classical *QoV*-based control system.

Two scenarios have been used to compare the control performances: (1) a road profile based on the standard ISO 8606 and, (2) a road that excites the vertical dynamics at different frequencies: *Bounce Sine Sweep* (BSS) test. A pick-up truck model in CarSim^{TM} is used as Software-in-the-Loop (*SiL*) in Matlab/Simulink^{TM}.

The paper is organized as follows. Next section presents the design of the heuristic controller based on the global suspension system. Section 3 shows the *QoV*-based heuristic controller. Results are presented in section 4. Finally, conclusions are in section 5. Table 1 describes all used variables.

⋆ This work was partially supported by *CONACyT* (PCP project 03/2010) and *Tecnológico de Monterrey* (Autotronics research chair)

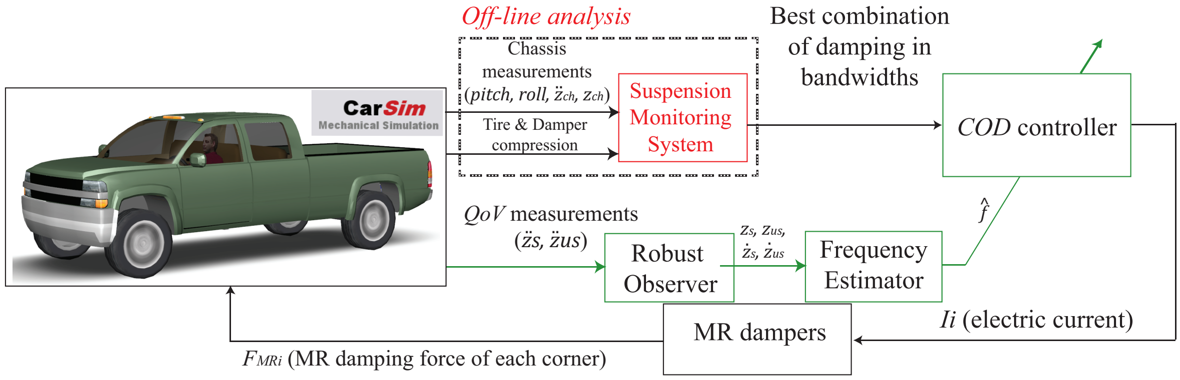

Fig. 1. Block diagram of the Combinatory quasi-Optimum Damping (COD) controller.

Table 1. Definition of Variables.

Variable	Description
$\lambda(\cdot)$	Weighting parameter, comfort vs road holding
a_i	Pre-yield viscous damping coefficient
b_i	Post-yield viscous damping coefficient
f_c	Dynamic yield force
$\hat{f}_{z_r}$	Estimated frequency of the road
F_{MR}	MR damper force
I	Electric current
k_s, k_t	Spring & wheel stiffness coefficient
m_s, m_{us}	Sprung & unsprung mass in the QoV
$x\|_a$	Index to monitor comfort, road holding
$X\|_{F_{MR_i}}$	COD index
z_{def}, $\dot{z}_{def}$	Position & velocity of the damper piston
z_r	Road profile
z_s, z_{us}	Vertical position of m_s, m_{us}
$\dot{z}_s, \dot{z}_{us}$	Vertical velocity of m_s, m_{us}
$\ddot{z}_s, \ddot{z}_{us}$	Vertical acceleration of m_s, m_{us}

2. GLOBAL SUSPENSION CONTROL SYSTEM

This kind of control is based on a full suspension system that involves the kinematics and compliance of the vehicle chassis, by integrating all related elements (springs, tires, stabilizer bars, dampers, etc.). The coupling nonlinear effects are included into the translational and rotational motions of the center of gravity. In an heuristic suspension controller, these nonlinearities are considered into the control law as measurements/estimations, such as: vertical chassis acceleration, heave displacement, pitch angle and roll angle.

The COD control strategy design is divided in two sections: (1) an off-line analysis in the frequency domain of the suspension system and (2) an on-line algorithm that computes the best damping combination (among the four MR dampers) according to the current driving conditions. Figure 1 shows the interaction between the off and on-line task [Tudón-Martínez et al., 2012].

The off-line analysis considers the suspension monitoring system, which analyzes the behavior of the vehicle chassis and wheels in the frequency domain when this is driven over a straight road profile whose roughness has enough frequency contents. The main idea is to analyze the vertical dynamics of the vehicle (acceleration, heave, roll and pitch for comfort and suspension deflection and tire deflection for road holding) in all damping combinations, in order to detect the best damping solution at each frequency of vibration.

By considering the most important states of a semi-active damper (low and high damping) [Nell and Steyn, 1998], there exist 16 combinations of actuation for the four MR dampers in the global suspension system. For instance, the configuration $(0, 0, 0, 0)$ means that the four MR dampers have an electric current value of 0 A (low damping), $(1, 1, 1, 1)$ means that all dampers have 2.5 A (high damping), $(1, 1, 0, 0)$ means the front dampers are on (2.5 A) and the rear dampers are off (0 A), and so on.

The analysis of the vertical dynamics with the 16 combinations of damping in the frequency domain allows the determination of the best damping combination for specific frequency bands. A BSS test at constant vehicle velocity is a good option to monitor the semi-active suspension system in the whole range of frequencies of interest in an automotive application.

Based on the hybrid control strategy of [Ahmadian, 1997], the COD controller selects the best damping solution according to the suspension monitoring system, by weighting the comfort and road holding control goals as:

$$X\,|_{F_{MR_i}} = \lambda(f_{z_r}) \cdot x\,|_{comf} + [1 - \lambda(f_{z_r})] \cdot x\,|_{rh} \qquad (1)$$

where, $X\,|_{F_{MR_i}}$ is a weighting index between the comfort and road holding in the i_{th} damping combination. $\lambda(f_{z_r})$ is the weighting parameter that depends on the excitation frequency; at low frequencies is desirable to have good comfort (i.e. for $f_{z_r} \leq 4$ Hz, $\lambda \geq 0.5$) and at high frequencies it is mandatory to ensure the road holding (i.e. for $f_{z_r} > 4$ Hz, $\lambda < 0.5$).

The comfort ($x\,|_{comf}$) or road holding index ($x\,|_{rh}$) monitors the semi-active suspension performance in bandwidths by using the passive suspension system as reference:

$$x\,|_a = \frac{1}{N} \sum_{j=1}^{N} \left. \frac{Var_j(MR_i)}{Var_j(passive)} \right|_{f_{z_r}} \qquad (2)$$

where, $a = \{comf, rh\}$ and Var_j is the frequency response magnitude/amplitude of the variable of interest during the test; that is, $x\,|_{comf}$ is the average index among the following j variables: roll, pitch, heave and vertical acceleration (N=4) by including the vertical force coupling among the four-wheel independent stations; whereas $x\,|_{rh}$ is the average among the suspension deflection and tire compression of the four corners (N=8). MR_i refers to the i_{th} damping combination under analysis and *passive* refers to the original suspension system by using a set of passive dampers. Thus, the quasi-optimum damping combination will be the configuration that minimizes the eqn. (1). This minimum index represents the best possible solution that improves comfort and ensure the wheel-road contact at each frequency of excitation when the pick-up truck is driven in a straight way.

Once the suspension monitoring system defines off-line the best damping solution for different frequencies band by using a *look-up* table, the *COD* controller dynamically determines on-line the configuration of the electric current for each *MR* damper (I_i) that is associated with the best damping solution according to the current vertical dynamics (i.e. frequency of motion), where i ={front-left, front-right, rear-left, rear-right}.

The on-line algorithm is as follows:

(1) Estimation of the frequency of motion by using the dynamics of a QoV model, by assuming that the road irregularities are uniform in all wheels.
(2) Selection of low (0 A) or high (2.5 A) damping at each wheel-station according to the pre-defined *look-up* table by the suspension monitoring system.

Figure 2 shows a block diagram to represent the algorithm that defines the *COD* controller output.

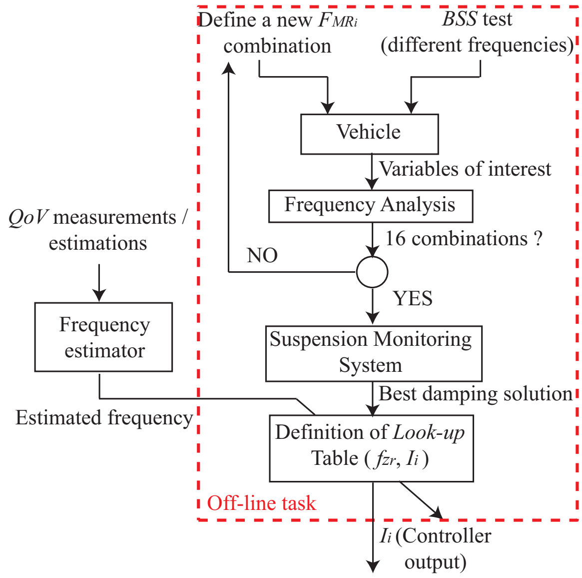

Fig. 2. Algorithm used to define the *COD* controller output.

3. QOV-BASED SUSPENSION CONTROL SYSTEM

This approach is similar to the global suspension control system; however, each wheel-station has an independent suspension monitoring system, frequency estimator and controller (*IHC*). Figure 3 shows a conceptual diagram of the suspension control system by considering independent wheel-stations.

In this case the suspension monitoring system analyzes the frequency response of the sprung mass acceleration (comfort) and the tire deflection (road holding), i.e. in the indexes $x\,|_{comf}$ and $x\,|_{rh}$, eqn. (2), $N = 1$. By considering only two levels of damping (low damping at 0 A or high damping at 2.5 A) in each *MR* damper, the minimum of eqn. (1) represents the best possible solution for this particular QoV model. Each QoV model uses a robust observer to estimate the frequency of the road profile.

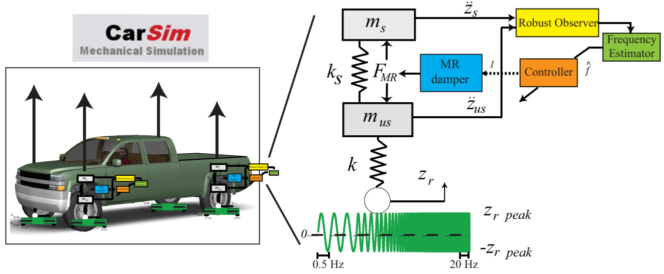

Fig. 3. Block diagram of an Indepndent Heuristic Controller (*IHC*).

The frequency content of the road irregularities can be estimated from the variables related to the suspension motion ($z_{def} = z_s - z_{us}$ and $\dot z_{def} = \dot z_s - \dot z_{us}$); however, because these variables are not easy to measure, an $\mathcal{H}_\infty$ robust observer is proposed to estimate them, by using a QoV model given by:

$$\underbrace{\begin{bmatrix}\dot z_s\\ \ddot z_s\\ \dot z_{us}\\ \ddot z_{us}\end{bmatrix}}_{\dot x} = \underbrace{\begin{bmatrix}0&1&0&0\\ \frac{-k_s}{m_s}&0&\frac{k_s}{m_s}&0\\ 0&0&0&1\\ \frac{k_s}{m_{us}}&0&\frac{-k_s-k_t}{m_{us}}&0\end{bmatrix}}_{A}\underbrace{\begin{bmatrix}z_s\\ \dot z_s\\ z_{us}\\ \dot z_{us}\end{bmatrix}}_{x} + \underbrace{\begin{bmatrix}0&0\\ \frac{-1}{m_s}&0\\ 0&0\\ \frac{1}{m_{us}}&\frac{k_t}{m_{us}}\end{bmatrix}}_{B}\underbrace{\begin{bmatrix}F_{MR}\\ z_r\end{bmatrix}}_{u} \tag{3}$$

$$\underbrace{\begin{bmatrix}\ddot z_s\\ \ddot z_{us}\end{bmatrix}}_{y} = \underbrace{\begin{bmatrix}\frac{-k_s}{m_s}&0&\frac{k_s}{m_s}&0\\ \frac{k_s}{m_{us}}&0&\frac{-k_s-k_t}{m_{us}}&0\end{bmatrix}}_{C}\begin{bmatrix}z_s\\ \dot z_s\\ z_{us}\\ \dot z_{us}\end{bmatrix} + \underbrace{\begin{bmatrix}\frac{-1}{m_s}&0\\ \frac{1}{m_{us}}&\frac{k_t}{m_{us}}\end{bmatrix}}_{D}\begin{bmatrix}F_{MR}\\ z_r\end{bmatrix} + \underbrace{\begin{bmatrix}v_1\\ v_2\end{bmatrix}}_{v}$$

where v models the noise in the accelerometers of the sprung ($\ddot z_s$) and unsprung masses ($\ddot z_{us}$).

An $\mathcal{H}_\infty$ robust observer is designed to be unsensitive to measurements noise and robust to unknown road profiles. The weighting functions W_{e_i} are used to minimize the estimation error of the state variables and W_{zr} shapes the road irregularities in the frequency range of interest for the suspension motion:

$$W_{zr} = \frac{K_{zr}\omega_{zr}s}{s+\omega_{zr}} \quad W_{e_i} = \frac{\zeta_{e_{1_i}}^2 s^2+2\zeta_{e_{1_i}}\omega_{e_{1_i}}s+\omega_{e_{1_i}}^2}{s^2+2\zeta_{e_{2_i}}\omega_{e_{2_i}}s+\omega_{e_{2_i}}^2} \tag{4}$$

By considering the filtering specifications, the generalized system $\mathcal{P}$ used for the synthesis of the $\mathcal{H}_\infty$ observer is given by eqn. (5). Figure 4 shows the structure of its design.

$$\mathcal{P} := \begin{cases} \dot x = A\cdot x + B\cdot w\\ \tilde y = C_2\cdot x + D_2\cdot w\\ z = (x-\hat x)\cdot [W_{e_1}W_{e_2}W_{e_3}W_{e_4}]^T \end{cases} \tag{5}$$

where $w = \begin{bmatrix}F_{MR}\\ W_{zr}\cdot \tilde z_r\end{bmatrix}$, $C_2 = \begin{bmatrix}C\\ 0_{1\times 4}\end{bmatrix}$, $D_2 = \begin{bmatrix}D\\ 1\ 0\end{bmatrix}$ and,

Table 2. Look-up table of the *COD* controller.

Specification	Bandwidth of control				
	B1	B2	B3	B4	B5
$\hat{f}_{z_r}$ [Hz]	$0-2$	$2-4$	$4-6$	$6-16$	>16
Quasi-optimum option	(1100)	(1111)	(0000)	(1111)	(1100)
Significant improvement	Heave & Vertical acc.	Pitch, suspension deflection & jounce in rear axle	Pitch & heave	Jounce rear axle, compression tire & suspension deflection	Vertical acc, heave & susp. deflection

$$\dot{\hat{x}} = A_{obs} \cdot \hat{x} + B_{obs} \cdot [\, \ddot{z}_s \;\ddot{z}_{us}\; F_{MR}\,]^T \tag{6}$$

such that A_{obs} and B_{obs} reduce the effect of the measurement noise and avoid drifting in the estimated variables by decreasing asymptomatically the error dynamics, given by $e\ (= x - \hat{x})$.

The observer is quadratically stable by solving an optimization problem with *Linear Matrix Inequalities* (*LMI*) techniques, [Scherer et al., 1997].

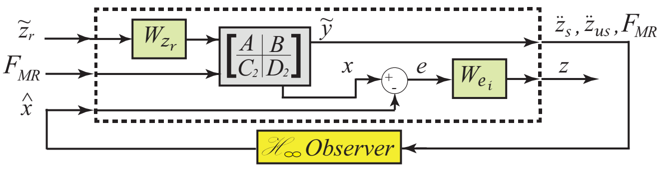

Fig. 4. $\mathcal{H}_\infty$ observer design in a *QoV* system.

By using the estimated states of the $\mathcal{H}_\infty$ observer, the road profile can be estimated from the static equation of the unsprung mass acceleration, as:

$$\hat{z}_r = [m_{us}\ddot{z}_{us} - k_s(\hat{z}_s - \hat{z}_{us}) + k_t\hat{z}_{us} - F_{MR}] \cdot k_t^{-1} \tag{7}$$

where F_{MR} is measured or modeled.

According to the ISO 8608, a road profile satisfies a sinusoidal wave whose frequency depends on the vehicle velocity and road quality. Thus, by assuming an harmonic motion in z_r, this unknown input could be given in a time instant by:

$$\hat{z}_r \approx R \cdot sin(\omega \cdot t) \qquad \dot{\hat{z}}_r \approx \omega \cdot R \cdot cos(\omega \cdot t) \tag{8}$$

where there is no feasible prior information of ω, which depends on: the road surface, tire dynamics and vehicle velocity. By using the effective *Root Mean Square* (*RMS*) value to sum two or more sinusoidal waveforms, the road profile frequency $\hat{f}_{z_r}$ can be estimated by the *RMS* values of the position and velocity of the road as:

$$\hat{f}_{z_r} = \dot{z}_{r_{RMS}} / (2 \cdot \pi \cdot z_{r_{RMS}})\ [Hz] \tag{9}$$

or in discrete *RMS* values of $\dot{z}_{r_{RMS}}$ and $z_{r_{RMS}}$:

$$\hat{f}_{z_r} = \sqrt{\frac{(\dot{z}_{r_1}^2 + \dot{z}_{r_2}^2 + \cdots + \dot{z}_{r_n}^2)}{(z_{r_1}^2 + z_{r_2}^2 + \cdots + z_{r_n}^2) \cdot 4\pi^2}} \tag{10}$$

where, n is the number of samples of a time window that guarantees at least 2 cycles of the estimated frequency.

By defining a *look-up* table in each *QoV* station, each *IHC* determines on-line the configuration of electric current in the *MR* damper that is associated to the best damping solution for the corresponding corner. The on-line algorithm to define the electric current in each corner is:

(1) Estimation of the state variables of the *QoV* model by using an $\mathcal{H}_\infty$ observer.
(2) Estimation of the road profile by using eqn. (7).
(3) Estimation of the frequency of motion in each *QoV* eqn. (10)
(4) Selection of low (0 A) or high (2.5 A) damping by using the pre-defined *look-up* table.

Experimental data obtained by a *K & C* test over a commercial pick-up truck have been used to model the vertical dynamics of the vehicle in CarSim^{TM}. The K_{erb} weight is 2,011 Kg, the rear unsprung mass is 280 Kg and the front one is 163 Kg. In a front *QoV* system the sprung mass is 630 Kg while for the rear is 387 Kg. The spring stiffness in each corner is non-linear; while the tire stiffness is considered constant: 230 N/mm.

The vehicle model is used as *SiL* in the Matlab/Simulink^{TM} platform. The experimental *MR* damper model, used in each corner, has been characterized according to the methodology described in [Lozoya-Santos et al., 2012] by using the parametric model proposed in [Guo et al., 2006]:

$$F_{MR} = I f_c \tanh(a_1\dot{z}_{def} + a_2 z_{def}) + b_1\dot{z}_{def} + b_2 z_{def} \tag{11}$$

whose identified parameters are: $f_c = 951.50$, $a_1 = 21.38$, $a_2 = 14.82$, $b_1 = 4,630.20$ and $b_2 = -3,948.60$.

4. SIMULATION RESULTS

A *BSS* test at 30 Km/h has been used to analyze the vertical dynamics between 0-15 Hz, the road elevation is decreased from 0.1 to 0.01 m. By using the suspension monitoring system, the *look-up* Table 2 shows the best damping solution in five frequency bands and highlights the variables with the best improvement when the *COD* controller is implemented.

For the *IHC*, the same *BSS* test is used to analyze the frequency response of each *QoV* model. After a frequency analysis of the variables of interest when $I = 0$ and 2.5 A, the *look-up* Table 3 summarizes the best electric current profile for comfort and road holding, by using 4 frequency bands.

Table 3. Look-up table for the *IHC*.

	Front *QoV*			
$\hat{f}[=]Hz$	0-2.5	2.5-4.5	4.5-12	12-20
$I[=]A$	2.5	0	2.5	0
	Rear *QoV*			
$\hat{f}[=]Hz$	0-2	2-6	6-14	14-20
$I[=]A$	2.5	0	2.5	0

Simulation results (Test 1 and 2) in the time domain are presented to compare the control performances of both approaches.

4.1 Test 1: Standard road ISO 8606 type F at 100 Km/h

Plots in Fig. 5 show the transient response of both suspension control systems respect to the baseline suspension system; the benefits of a semi-active suspension in the vertical dynamics are clear. The road elevation that represents a standard road profile type F according to the ISO 8606 (poor quality) is shown in Fig. 5A. For comfort, the two control systems reduce the pitch angle up to 3 degrees, Fig. 5B; the vertical acceleration up to 5 g's, Fig. 5C; the vertical displacement up to 0.3 m , Fig. 5D; and the roll angle up to 1.5 degrees, Fig. 5E. For road holding, the jounce motion of the rear solid axle is reduced up to 100 mm with the suspension controllers, Fig. 5F; the tire compression (front-left) up to 200 mm of displacement, Fig. 5G; and the damper compression (front-left) up to 100 mm at different time instants (similar results are obtained in a rear damper). Both controllers can manage the trade-off between comfort and road holding.

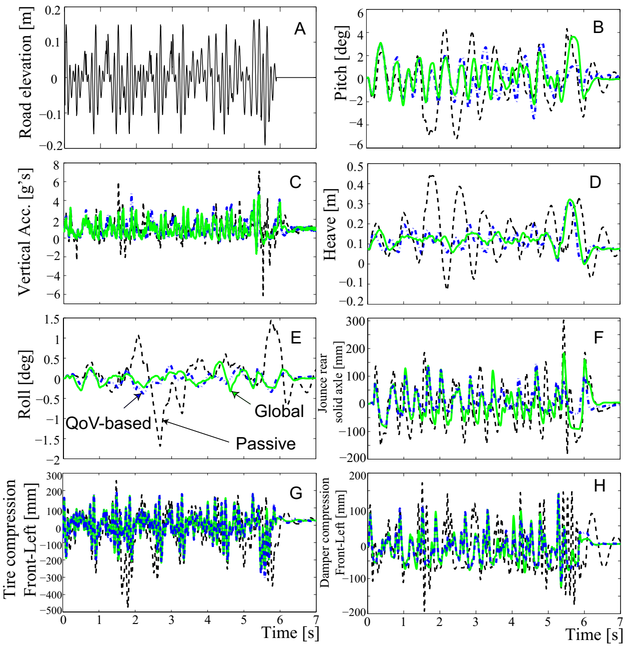

Fig. 5. Performance of the suspension control systems in a ISO road test; passive system (black dashed line), Global controller: *COD* (green continuous line) and *QoV*-based control: *IHC* (blue dashed line).

4.2 Test 2: BSS test (amplitude: 0.1 to 0.01 m) at 30 Km/h

This road test allows the analysis of the vertical dynamics at different excitation frequencies, Fig. 6A. The comparison of the control performances between the suspension control systems shows that, the motion of the vehicle body (Fig. 6B-D) is lower with the global suspension controller, specially between 7 and 17 s when the frequency of motion is between 2 and 3 Hz. It is important to note that the absence of coordination between the independent controllers causes an insufficient comfort performance; e.g. the roll angle is significantly increased due to this absence of coordination.

Figure 6E shows that the road holding is higher when the suspension controller is *QoV*-based, e.g. the jounce motion of the rear solid axle, which is directly related to the vertical motion of the rear wheels, it is significantly reduced with the *IHC* approach. Therefore, the *QoV*-based control system is more sensitive to vibrations of the unsprung mass.

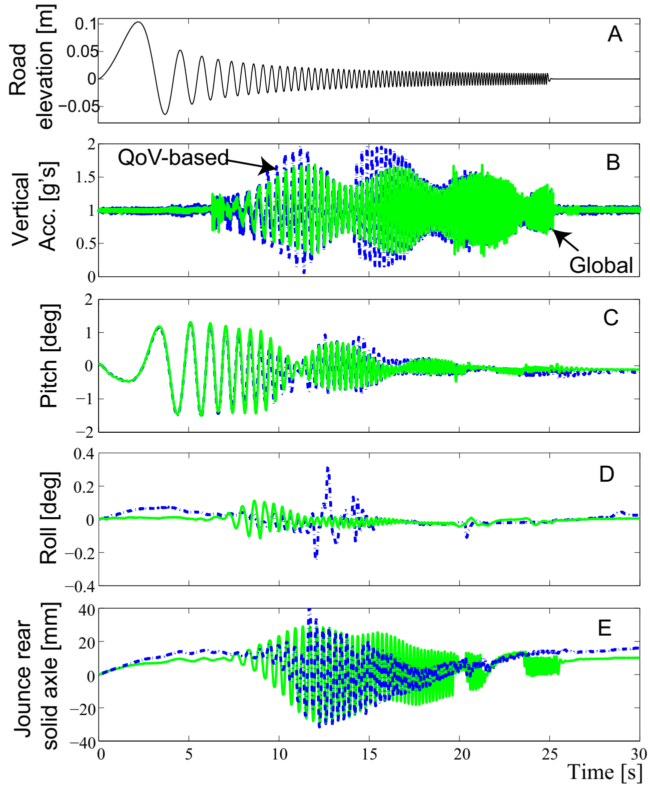

Fig. 6. Suspension control systems performance in the *BSS* test. Global controller: *COD* (green continuous line) and *QoV*-based control: *IHC* (blue dashed line).

The *RMS* value of the variables of interest is used as performance index to quantify the control performances of both suspension control systems with respect to the passive system, according to:

$$p = \frac{RMS_{Controller}}{RMS_{Passive}} \tag{12}$$

where, p monitors the improvement degree of the suspension control system during the test, it is desirable for p to tend to 0.

Table 4 shows that the global suspension control system has better comfort performance for both simulation tests, i.e. the semi-active suspension control is well coordinated by including all mechanical joints between the wheel-stations. For instance, the roll angle is improved up to 70% with respect to the passive suspension system, the pitch angle 35% and the vertical displacement 33%.

For road holding, the *QoV*-based controller shows better performance. The major improvement is observed in the suspension deflection, i.e. lower compression in the dampers (reduction up to 44%) and smaller jounce in the rear solid axle (reduction around 43%).

From the practical point of view, the *QoV*-based control system needs at least eight acceleration sensors and four microcontrollers to be implemented; while, the global suspension control system needs 4 sensors (3 accelerometers and 1 gyroscope multi-axle) and one microcontroller, i.e. less instrumentation. The main limitation of both controllers is the sampling frequency, the sampling time must ensure the collection of the necessary data to reconstruct 2 periods of signals of interest in order to estimate the frequency of motion.

Table 4. Control Performances in the (ISO road, BSS) tests respect to the passive system

Comfort performance					
Susp Control Sys	Heave	Roll	Pitch	Vert Acceleration	
QoV-based	{0.74, **0.97**}	{0.40, 1.22}	{0.76, **0.95**}	{**0.95**, 1.00}	
Global	{**0.67**, **0.97**}	{**0.30**, **0.66**}	{ **0.65**, **0.95**}	{0.98, 0.**98**}	
Road holding performance					
Suspension Control System	Damper Compression front QoV	Damper Compression rear QoV	Tire Compression front QoV	Tire Compression rear QoV	Jounce rear solid axle
QoV-based	{**0.58**, **0.68**}	{**0.56**, 0.98}	{0.69, **1.00**}	{**1.00**, **1.00**}	{**0.57**, **0.92**}
Global	{0.69, 0.76}	{0.76, **0.92**}	{**0.67**, **1.00**}	{**1.00**, **1.00**}	{0.77, 0.98}

The synchronization of the control laws for the different goals and optimization of the frequency estimator algorithm are part of the future work.

5. CONCLUSIONS

A comparison between two heuristic control schemes for a semi-active suspension system has been presented: (1) a global suspension control system that includes the coupling among the four vertical forces and (2) a suspension system composed by 4 independent controllers, one for each *Quarter of Vehicle* (QoV) model. Both controllers use a monitoring system of the vertical dynamics to establish a static control law for comfort and road holding. The comparison was carried on a pick-up truck model in CarSim^{TM}, equipped with magneto-rheological dampers modeled from experimental data.

The objective is to highlight the advantages and implications of a global suspension controller that coordinates the four vertical forces in contrast to the classical QoV-based controller.

Two different running tests on the road have been used to compare the control performances when the vehicle is driven in straight trajectories.

Simulation results show that both control strategies manage the trade-off between comfort and road holding in comparison to a passive suspension system. In general, when the suspension control system includes the load transfer coordination between the corners, the comfort performance is greater, e.g. the vertical chassis displacement is reduced 33% and the pitch motion 35%. However, the QoV-based controller is more sensitive to the unsprung mass motions, and thus it shows a major reduction on road holding, e.g. the jounce in the rear solid axle is improved up to 43%. In this case, both control designs have similar complexity because both depend on measurements; but, more instruments are needed when 4 independent controllers are used.

REFERENCES

M. Ahmadian. A Hybrid Semiactive Control for Secondary Suspension Applications. In *ASME-ICE, Symp on Advanced Automotive Tech*, pages 743–750, 1997.

M. Chadli, A.E. Hajjaji, and A. Rabhi. h_∞ observer-based robust multiple controller design for vehicle lateral dynamics. In *American Control Conf*, pages 1508–1513, 2010.

S.B. Choi, H.S. Lee, and Y.P. Park. H_∞ Control Performance of a Full-vehicle Suspension Featuring Magnetorheological Dampers. *Vehicle System Dynamics*, 38 (5):341–360, 2002.

C. Crivellaro. Robust Semi-active Suspension System Control for Pickup Truck. In *SAE World Congress & Exposition*, 2009.

X. Dong, M. Yu, Z. Li, C. Liao, and W. Chen. Neural Network Compensation of Semi-active Control for a Magneto-rheological Suspension with Time Delay Uncertainty. *Smart Materials and Structures*, 18:1–14, 2009.

S. Guo, S. Yang, and C. Pan. Dynamical Modeling of Magneto-rheological Damper Behaviors. *J. of Intell. Mater., Syst. and Struct.*, 17:3–14, 2006.

S. Ikenaga, F.L. Lewis, J. Campos, and L. Davis. Active Suspension Control of Ground Vehicle Based on a Full-vehicle Model. In *American Control Conf*, pages 4019–4024, 2010.

J.J. Lozoya-Santos, R. Morales-Menendez, R.A. Ramirez-Mendoza, J.C Tudon-Martinez, O. Sename, and L. Dugard. Magnetorheological Damper - An Experimental Study. *J. of Intelligent Mater. Syst. and Struct.*, 23:1213–1232, 2012.

S. Nell and J.L. Steyn. An Alternative Control Strategy for Semiactive Dampers on Off-road Vehicules. *J. of Terramechanics*, 35(1):25–40, 1998.

C. Poussot-Vassal, C. Spelta, O. Sename, S.M. Savaresi, and L. Dugard. Survey and Performance Evaluation on Some Automotive Semi-Active Suspension Control Methods: A Comparative Study on a Single-corner Model. *Annual Reviews in Control*, 36(1):148–160, 2012.

C. Scherer, P. Gahinet, and M. Chilali. Multiobjective Output-feedback Control Via LMI Optimization. *IEEE Trans. on Automatic Control*, 42(1):896–911, 1997.

J. Swevers, C. Lauwerys, B. Vandersmissen, M. Maes, K. Reybrouck, and P. Sas. A Model-free Control Structure for the On-line Tuning of the Semi-active Suspension of a Passenger Car. *Mechanical Systems and Signal Processing*, 21(3):1422–1436, 2007.

J.C. Tudón-Martínez, J.J. Lozoya-Santos, C.A. Vivas, R. Morales-Menendez, and R. Ramirez-Mendoza. Model-free Controller for a Pick-up Semi-active Suspension System. In *ASME Int. Mechanical Eng. Congress & Exposition*, pages 67 –76, Texas USA, 2012.

J. Wang, D.A. Wilson, W. Xu, and D.A. Crolla. Active Suspension Control to Improve Vehicle Ride and Steady-State Handling. In *44^{th} IEEE Conf. on Decision and Control and European Control Conf.*, pages 1982–1987, 2005.

J. Yoon, W. Cho, J. Kang, B. Koo, and K. Yi. Design and Evaluation of a Unified Chassis Control System for Rollover Prevention and Vehicle Stability Improvement on a Virtual Test Track. *Control Eng. Practice*, 18(6): 585–596, 2010.